Atmos. Chem. Phys. Discuss., 7, 10043–10063, 2007
www.atmos-chem-phys-discuss.net/7/10043/2007/
© Author(s) 2007. This work is licensed
under a Creative Commons License.

Atmospheric Chemistry and Physics Discussions

Air-to-sea flux of soluble iron: is it driven more by HNO_3 or SO_2? – an examination in the light of dust aging

H. Yang and Y. Gao

Department of Earth and Environmental Sciences, Rutgers University, Newark, New Jersey 07102, USA

Received: 15 June 2007 – Accepted: 4 July 2007 – Published: 11 July 2007

Correspondence to: Y. Gao (yuangaoh@andromeda.rutgers.edu)

Abstract

Aeolian dust provides the major micronutrient of soluble Fe to organisms in certain regions of the global ocean. In this study, we conduct numerical experiments using the MOZART-2 atmospheric chemistry transport model to simulate the global distribution of soluble Fe flux and Fe solubility. One of the mechanisms behind the hypothesis of acid mobilization of Fe in the atmosphere is that the coating of acidic gases changes dust from hydrophobic to hydrophilic, a prerequisite of Fe mobilization. We therefore include HNO_3, SO_2 and sulfate (SO_4^{2-}) as dust transformation agents in the model. General agreement in Fe solubility within a factor of 2 is achieved between model and observations. The total flux of soluble Fe to the world ocean is estimated to be 731–924×10^9 g yr^{-1}, and the average Fe solubility is 6.4–8.0%. Wet deposition contributes over 80% to total soluble Fe flux to most of the world oceans. Special attention is paid to the relative role of HNO_3 versus SO_2 and sulfate. We demonstrate that coating by HNO_3 produces over 36% of soluble Fe fluxes compared to that by SO_2 and sulfate combined in every major oceanic basin. Given present trends in the emissions of NO_x and SO_2, the relative contribution of HNO_3 to Fe mobilization may get even larger in the future.

1 Introduction

Iron (Fe) limits primary productivity in oceanic regions characterized by high-nitrate and low-chlorophyll (HNLC) (Martin, et al., 1994; Coale et al., 2004). Fe may also affect many oceanic biological processes, including nitrogen fixation (Falkowski, 1997). The major source of Fe in the open ocean is soil dust transported from the atmosphere (Duce et al., 1991; Fung et al., 2000), although other processes, such as upwelling of deep water, also contribute (Coale et al., 1996; Meskhidze et al., 2007). Because only soluble Fe is readily available to phytoplankton, it is critically important to know the solubility of aeolian Fe, which acts as a connection between desert dust and ocean

ACPD

7, 10043–10063, 2007

biogeochemistry (Gao et al., 2003; Jickells et al., 2005).

Meskhidze et al. (2003, 2005) simulated Fe solubility by assuming that dust aerosols deliquesced in the first place. Fan et al. (2006) proposed a two-step mechanism, which assumes that Fe dissolution (the second step) is initiated only after a certain amount of water-soluble acids coated on dust (the first step). The acid coating increases the water-absorbing capacity of dust, since fresh dust absorbs too little water vapor to form solutions on the dust surface (Goodman et al. 2000; Vlasenko et al. 2006). The Fe dissolution rate is prescribed when the coating is controlled by HNO_3 and SO_2 in Fan et al. (2006). Considering that future air quality control will have different impacts on NO_x (the precursor of HNO_3) and SO_2 emissions (IPCC 2001, A2p), it is important to examine the relative contribution of HNO_3 and SO_2 to Fe solubility through dust aging. Consequently it becomes critical to know the most important parameters to measure and to include in the model. Sulfate (SO_4^{2-}) is formed by conversion of SO_2, and it has a higher concentration than SO_2 over the ocean and over continental areas away from the SO_2 source regions. We therefore include coagulation of sulfate in dust transformation as well, and compare its effect together with the SO_2 coating to that by HNO_3 coating.

This study aims to quantify the relative importance of HNO_3 and SO_2 (including sulfate) to soluble Fe fluxes to the ocean through numerical model simulations. Section 2 describes the heterogeneous uptake of HNO_3 and SO_2 on dust, the coagulation of sulfate with dust, and the parameterization of Fe dissolution rates. Section 3 presents the simulated Fe solubility plus its comparison with in situ observations. The relative contribution by HNO_3 is calculated, and sensitivity tests are performed at the lower limits of γ_{HNO_3} and γ_{SO_2}. Discussions are presented with respect to relevant observations and other modeling studies concerning Fe solubility, followed by Sect. 4, a summary of the major conclusions.

ACPD
7, 10043–10063, 2007

2 Method

We use the MOZART-2 atmospheric transport model to simulate the Fe solubility. The meteorology fields are provided by NCEP reanalysis (Kalnay et al., 1996), with 28 vertical layers and a horizontal resolution as 1.9°×1.9°. The chemistry module (Horowitz et al., 2003; Tie et al., 2005) simulates 90 species, including SO_2, NO_x, HNO_3, sulfate and dust aerosols. In addition, dust in each of the 5 size bins is classified into three categories: fresh, coated, and "dissolved" as in Fan et al. (2006). Higher wet removal rates are prescribed for coated and "dissolved" dust than for fresh dust due to the hydrophilic characteristics after dust transformation (Fan et al., 2004). The transformation of dust from fresh to coated is controlled by heterogeneous uptake of gases (HNO_3 and SO_2) and the coagulation of sulfate on dust, and the transformation of dust from coated to "dissolved" is controlled by the dissolution rate of Fe. The model was run for the year of 2001.

The uptake coefficient (γ) is a critical parameter controlling the gas transfer rate. There is a large uncertainty in γ since it is very sensitive to aerosol surface properties (JPL Publication 02-25). Table 1 lists the values of γ used in this study. The Base case has the median values of γ where γ_{HNO_3} is ~10 times of γ_{SO_2}. The Ref case has the lower limits of γ where γ_{HNO_3} and γ_{SO_2} have the same magnitudes. We do not include the case with the upper limits of γ where γ_{HNO_3} is ~100 times of γ_{SO_2} since HNO_3 already makes a larger contribution than SO_2 to Fe mobilization in the Base case as our results later indicate, and the gas concentrations of HNO_3 and SO_2 are reduced too heavily to be realistic in current MOZART settings.

The dust aging or transformation (κ_c , s^{-1}) from fresh to coated is by gas condensation (Eq. 1) and by sulfate coagulation (Eq. 2):

$$\kappa_g = \frac{\sum_j Kd_j C_j}{\delta m} \quad (1)$$

where Kd_j (m^3 s^{-1}) is the diffusion coefficient of gas j that is a function of γ; C_j is

ACPD
7, 10043–10063, 2007

EGU

the concentration of gas j (kg m^{-3}), and δm (kg) is the required coating mass for dust transformation with a thickness assumed to be 1 nm (Fan et al., 2006).

$$\kappa_{SO_4} = \frac{K_{12} N_1}{\delta N_1} \quad (2)$$

where the coagulation coefficient K_{12} is a function of both sulfate and dust particle sizes (Seinfeld and Pandis, 1998). N_1 and N_2 represent the particle number concentration of sulfate and dust, respectively. The required mass of coagulated sulfate ($\sim \delta N_1$) is assumed to be the same as the acidic coating by gases. The mass median diameter of sulfate aerosol is set at 0.31 μm and the geometric standard deviation at 2.03 (the grand continental average in Whitby, 1978). The transformation time τ_c(s) is the inverse of $\kappa_c = \kappa_g + \kappa_{SO_4}$.

Hematite (α-Fe_2O_3) is a major Fe oxide in soil (Cornell and Schwertmann, 2003), which is highly insoluble under alkaline conditions, and dissolves slowly in acid solution in the presence of light and ligands, compared to other forms of Fe oxides (Martin, 2005). The hematite dissolution rate is used for the calculation of Fe solubility in this study. The transformation rate κ_s (s^{-1}) of dust from coated to "dissolved" is the same as the dissolution rate of hematite or Fe:

$$\kappa_s = R_d A W_{Fe_2O_3} \quad (3)$$

where R_d is the hematite dissolution rate in mole per unit surface area, A is the specific hematite surface area, and $W_{Fe_2O_3}$ is the formula weight of hematite (159 g mol^{-1}). R_d is set as 4×10^{-11} mol m^{-2} s^{-1} and A is 100 m^2 g^{-1}, following Fan et al. (2006). One needs to scale the "dissolved" dust by 3.5% (Duce et al., 1991) to obtain the dissolved Fe. It is assumed in the model that 0.5% dust is coated and the same amount is "dissolved" when dust is emitted, which implies the lower limit Fe solubility as 0.5% in dust source regions.

The value of R_d of 4×10^{-11} mol m^{-2} s^{-1} was used to match the lower limit of γ in the Ref case as by Fan et al. (2006), which has a slower dust transformation than the Base

ACPD
7, 10043–10063, 2007

case. For faster dust transformation produced by larger γ as in the Base case, R_d as 4×10^{-11} mol m^{-2} s^{-1} produces a far larger Fe solubility compared to observations. R_d as 4×10^{-11} mol m^{-2} s^{-1} produces a high bias in Fe solubility in the Ref case as well, due probably to the online SO_2 and HNO_3 that generate a faster dust transformation in this study than in Fan et al. (2006), where monthly mean SO_2 and HNO_3 are used. Since Fe dissolution occurs in a solution, it is assumed in this study that Fe dissolves only when the ambient relative humidity (RH) is above a threshold RH_{sh}. RH_{sh} is 76% for the Base case and 45% for the Ref case, which are determined by trial and error to match the observations.

To have a quantitative understanding of the contribution by HNO_3 to soluble Fe flux, we ran three experiments for each case listed in Table 1. Experiment 1 has HNO_3, SO_2, and sulfate as the dust transformation agents, experiment 2 has HNO_3 as the coating gas, and experiment 3 has SO_2 and sulfate as the dust transformation agents. The model is constrained in experiment 1. Since dust aging and the Fe dissolution process are nonlinear, the addition of soluble Fe flux produced in experiments 2 and 3 is always larger than that in experiment 1, especially in locations far away from dust source regions or if the dust transformation is very fast. We therefore check the ratio of soluble Fe flux between experiment 2 and 3 (F_{23}), which explains the relative importance of HNO_3 compared to SO_2 and sulfate.

3 Results and discussion

3.1 Model validation and the global distribution of soluble Fe flux

We focus on the Base case first. Figure 1 shows that the simulated Fe solubility (with contributions from both gases and sulfate) has an overall good agreement with observations collected from 1988 to 2002, with 15 points scattered within a factor of 2 of the observed values and 4 points close to the 50% distance lines. The model generally captures the variation feature of the Fe solubility, which ranges from ~2% close to dust

ACPD
7, 10043–10063, 2007

EGU

source regions to ~35% in remote areas as validated recently for bulk dust simulation (Yang et al., 2007[1]).

Figure 2 depicts the global distribution of (a) soluble Fe flux and (b) Fe solubility over the ocean. The soluble Fe flux is the highest in the north Tropical Atlantic (>100 μmol m^{-2} yr^{-1}) where the Fe solubility is low (~5%), due to its proximity to the largest dust source region in North Africa. The same pattern is seen in the North Indian Ocean. The Tropical Pacific receives little soluble Fe flux (~20 μmol m^{-2} yr^{-1}) but has a high solubility (~25%), being far away from any major dust sources. North Pacific has a medium soluble Fe flux (~50 μmol m^{-2} yr^{-1}) and solubility (~16%), due to its modest distance from the dust source region in Asia and the dense air pollution in East Asia. The ocean in the southern hemisphere (SH) generally has a lower soluble Fe flux and solubility than the northern hemisphere (NH) due to weaker dust source strength and generally lower HNO_3 and SO_2 and sulfate concentrations. Table 2 gives the soluble Fe flux and Fe solubility in each major oceanic basin and the three major HNLC regions. The total air-to-sea soluble Fe flux is 731×10^9 g yr^{-1}, and the average Fe solubility over the ocean is 6.4%.

Wet deposition contributes >80% to soluble Fe flux over most of the world ocean (Gao et al., 2003; Fan et al., 2006), implying Fe mobilization generally undergoes precipitation processes besides being cycled through clouds (Junge, 1964). The Fe solubility is 3.1% and 7.9% in dry and wet deposition over the ocean in the NH (not including the Arctic), and it is 2.1% and 8.2% respectively in the SH. The smaller Fe solubility in dry deposition is mainly caused by the large amount of dry deposition near dust source regions, while most wet deposition occurs in remote areas where dust has stayed a much longer time in the atmosphere for a larger fraction of Fe to be mobilized (Yang et al., 2007[1]). The slower wet removal rate of fresh dust is another reason for the high Fe solubility in wet deposition (see Sect. 2). The smaller difference in Fe solubility between dry and wet deposition in the NH is probably due to the lower fraction of fresh

[1]Yang, H., Gao, Y., and Horowitz, L.: The size distribution of entrained dust and the impact on dust load and deposition to the ocean, J. Geophys. Res., submitted, 2007.

ACPD
7, 10043–10063, 2007

EGU

dust, which is <5% over most of the ocean, caused by the higher air pollution level and the subsequent faster dust transformation from fresh to coated. On the contrary, the fraction of fresh dust is between 10% and 80% in the SH, which makes the Fe solubility in dry deposition lower than in wet deposition.

3.2 The sensitivity to uptake coefficients of acid gases

Table 2 shows large differences in soluble Fe flux and solubility to the world ocean between the two cases where different uptake coefficients of acid gases are prescribed, and different RH_{sh} is adjusted accordingly. The soluble Fe flux in the Ref case is ~1.5 times that of the Base case in the North Atlantic and the North Indian Ocean. It is ~20% higher than the Base case in the North Pacific. Obviously, the increased effect of a smaller RH_{sh} in the Ref case outweighs the decreased effect of a slower dust transformation rate, which is caused by the dry climate and high air pollution level in the NH. The contrast is milder in the major oceanic basins in the SH, where the difference factor is generally within 10%, and it is reversed in the South Indian Ocean and the South Pacific. The comparison of Fe solubility between the two cases exhibits a similar pattern. The soluble Fe flux and Fe solubility over the Southern Ocean in the Base case is about twice that in the Ref case, which is caused by the slower dust transformation in the Ref case. As RH is generally higher than 80% in this region, the difference in RH_{sh} between the two cases does not produce a difference. The total air-to-sea soluble Fe flux is $924\times10^{9}\,g\,yr^{-1}$, and the average Fe solubility over the ocean is 8.0%.

The contribution by dry deposition to soluble Fe flux over most oceans is <20%, similar to the Base case. However, the difference in Fe solubility between dry and wet deposition is larger in the Ref case. It is 3.4% and 11% for dry and wet depositions respectively over the ocean in the NH, and is 1.6% and 8.1% in the SH. The main reason is probably the higher fraction of fresh dust than in the Base case, which is between 60–80% in the NH and over 80% in the SH, caused by the lower limits uptake coefficients of acid gases, and fresh dust has a lower wet removal rate than the aged

ACPD
7, 10043–10063, 2007

EGU

dust (see Sect. 2). The comparison of simulated Fe solubility and bulk dust in the Ref case has an overall good agreement with limited observations as well. Due to the sparse observations constraining the model, we propose to further explore this issue in the near future with more available data from more widely distributed in situ measurements of Fe solubility.

We compare our results with the Fe budget in the upper ocean proposed by Fung et al. (2000). By using the global primary productivity of 43.5 Pg yr^{-1} (Behrenfeld and Falkowski, 1997), and assuming a cellular Fe:C in phytoplankton ranging from 2.5–6.5 μmol mol^{-1} in the open ocean and 25 μmol mol^{-1} for the coastal region, Fung et al. (2000) estimated that the global Fe assimilation by phytoplankton in the ocean is 26×10^9 mol Fe yr^{-1} and the aeolian soluble Fe flux was estimated to be 11.8×10^9 mol Fe yr^{-1} (10% Fe solubility). The soluble Fe flux to the world ocean predicted in the Base case is 13.1×10^9 mol Fe yr^{-1} (731×10^9 g yr^{-1}), and it is 16.6x10^9 mol Fe yr^{-1} (924×10^9 g yr^{-1}) in the Ref case. The estimated soluble Fe flux is 15.8×10^9 mol Fe yr^{-1} in Luo et al. (2005), and it is 41.2×10^9 mol Fe yr^{-1} in Fan et al. (2006). Therefore our results are close to the lower end of the range in the literature.

3.3 Soluble Fe flux produced by HNO_3 versus that by SO_2 and sulfate

The global distribution of the annual mean ratio of soluble Fe flux produced by HNO_3 versus that by SO_2 and sulfate (F_{23}) in the Base case is presented in Fig. 3. F_{23} is higher than 1.0 over most world oceans, suggesting that HNO_3 makes a larger contribution to soluble Fe fluxes than SO_2 and sulfate. More specifically, in the NH, F_{23} is the highest over the North Atlantic (1.76), followed by the North Indian Ocean (1.66) and the North Pacific (1.36). F_{23} is similar among different oceanic basins in the SH. The factors affecting F_{23} in a certain area are the dust transformation rate by HNO_3 versus by SO_2 and sulfate, and the distance to its major dust source region. As our focus is on the first aspect, we hereby examine the relative magnitude of the conversion rates by HNO_3 versus by SO_2 and sulfate to interpret the distribution of F_{23}.

ACPD
7, 10043–10063, 2007

EGU

Calculations from this study show that at the surface level, HNO_3 generally has a higher conversion rate than SO_2 in major dust source regions in the NH, where over 90% dust is transformed from fresh to aged in the Base case. The transformation takes ~33 h by HNO_3 in the North Africa and the Arabian Peninsula, and ~26 h in the Central and East Asia. It takes ~887 and ~176 h by SO_2 respectively in these regions. The concentration of HNO_3 varies from ~0.1 to 1 ppb and ranges from ~10% to 200% of SO_2 in these regions. HNO_3 has a lower conversion rate than SO_2 in Europe, east China and east U.S., where the RH is much higher than in the dust source regions, with the concentration of SO_2 above 5 ppb and HNO_3 less than 10% of that. However, the fraction of fresh dust is less than 5% of total dust in these regions. The conversion rate by HNO_3 is higher than that by SO_2 almost everywhere in the free troposphere since the concentration of SO_2 decreases faster with height than HNO_3. The conversion by sulfate takes ~624 h in the North Africa and the Arabian Peninsula, and ~455 h in the Central and East Asia. It turns out that the dust transformation by HNO_3 is higher than that by SO_2 and sulfate together.

Similar arguments can be applied to the SH; however, at the surface level over the ocean the fraction of fresh dust ranges from ~10% to 80% of the total dust instead of ~5% in the NH, as the transformation is slower due to the lower concentration of HNO_3 than in the NH. Therefore, F_{23} in the South Indian Ocean (1.49) and South Atlantic (1.40) is lower than in the North Indian Ocean (1.66) and the North Atlantic (1.76). F_{23} in the Ref case is generally higher than in the Base case. This is because the overall dust transformation is much slower in the Ref case than in the Base case and therefore the single contributions are more "linear" and "addable" here (see Sect. 2). For example, at the surface level in the dust source region in North Africa, the average transformation rate in the Base case is ~10 times faster than in the Ref case.

The dust transformation rate in the Ref case is comparable to Fan et al. (2006), e.g. ~1 day for 2 ppb SO_2 + 1 ppb HNO_3, based on similar prescription of gas uptake coefficients. The gas removal rate on dust is on the order of $10^{-5}\,s^{-1}$ in dust source regions in the Base case, comparable to Dentener et al. (1996) that had a gas removal

ACPD
7, 10043–10063, 2007

EGU

rate as $10^{-3}\,s^{-1}$ with a prescribed γ of 0.1. Finally, the reduction of HNO_3 through heterogeneous uptake on dust ranges from 10% to 30% in high dust loading regions at the surface level, and it is generally <5% in remote areas in the Base case, which compares well with the special case in Bauer et al. (2004). SO_2 in dust source regions is reduced up to 80%, since condensation on dust provides the major sink of SO_2. The change of sulfate is in between. Thus our conclusion is robust even when considering the feedback of gas concentrations.

3.4 Other factors affecting Fe solubility

There are many factors affecting Fe solubility in the atmosphere besides HNO_3, SO_2 and sulfate (we will refer to SO_2 alone hereafter), such as some organic acids that can form complexes with Fe, and the pH of the aerosol solution. For instance, the Fe dissolution rate could be the same at pH=5 in the presence of oxalate as the one at pH=2 in the absence of oxalate (Cornell and Schwertmann, 2003; Martin 2005). HNO_3 and SO_2 could also directly increase the Fe dissolution rate (the second step of the two-step mechanism) by reducing the pH of the aerosol solution, in which case SO_2 may play a more important role than HNO_3 (Meskhidze et al., 2003, 2005). This study examines the relative contribution of HNO_3 and SO_2 to Fe solubility through dust aging, the first step to dissolve Fe, by fixing the Fe dissolution rate. A more sophisticated parameterization of Fe dissolution will be conducted as the next step to explore new insights for a better understanding of Fe solubility.

Nevertheless, our method is supported by the major conclusions of several other modeling studies. Hand et al. (2004) and Luo et al. (2005) examined the correlation between simulated and observed Fe solubility by studying the effects of photoreduction, cloud processing, SO_2, pH, sulfate aerosol and organic carbonaceous aerosol. Only cloud processing, among the six processes, is found to have an overall correlation larger than 0.2, and SO_2 is the next with a high correlation (Luo et al. 2005). The use of a threshold RH_{sh} of 76% for Fe dissolution in the Base case is close to being

ACPD
7, 10043–10063, 2007

EGU

able to include cloud processing, and the two-step mechanism allows us to include the effect of HNO_3 and SO_2on dust aging at the same time. An implicit assumption in our method that the dissolved Fe remains under-saturated in the deliquesced dust solution is supported by Meskhidze et al. (2005), who examined the speciation of the dissolved Fe. And our conclusion is supported by recent observations by Ooki and Uematsu (2005), who demonstrated that nitrate was the dominant acid associated with mineral dust particles rather than non-sea salt (nss)-sulfate. They also observed through an in situ experiment that HNO_3 reacted with dust much more efficiently than SO_2. Observations made over the remote ocean showed that there is more nitrate internally mixed with dust than nss-sulfate (Zhu et al., 1992), although some nitrate might have been replaced by sulfate during cloud processing (Seinfeld and Pandis, 1998). Those findings provide additional justification to highlight the importance of HNO_3 in dissolution of Fe from mineral dust.

4 Summary

Our results show that HNO_3 makes a larger contribution to Fe mobilization than SO_2 through dust aging in the atmosphere. In addition, the concentrations of HNO_3 and SO_2 are closely related to their precursors (NO_x for HNO_3) or emission sources, since both are short-lived gases (~1 week in the troposphere). IPCC 2001 (A2p) predicted the emission of NO_x to increase 4 times, and the emission of SO_2 to decrease slightly in the next 100 years. We therefore suggest that the iron fertilization to oceanic biology caused by air pollution is going to continue even if the fertilization caused by SO_2 decreases in the future.

Acknowledgements. We would like to thank L. Horowitz for support of using MOZART-2. We thank P. Falkowski for valuable comments. Discussions with H. Levy were helpful. NOAA/GFDL provided the computer resources for running MOZART-2. This work is supported by the NASA award NNG04G091G.

References

Bauer, S. E., Balkanski, Y., Schulz, M., Hauglustaine, D. A., and Dentener, F.: Global modeling of heterogeneous chemistry on mineral aerosol surfaces: Influence on tropospheric ozone chemistry and comparison to observations, J. Geophys. Res., 109, D02304, doi:10.1029/2003JD003868, 2004.

Behrenfeld, M. J. and Falkowski, P. G.: Photosynthetic rates derived from satellite-based chlorophyll concentration, Limnol. Oceanogr., 42, 1–20, 1997.

Buck, C. S., Landing, W. M., Resing, J. A., and Lebon, G. T.: Aerosol iron and aluminum solubility in the northwest Pacific Ocean: Results from the 2002 IOC cruise, Geochem. Geophys. Geosyst., 7, Q04M07, doi:10.1029/2005GC000977, 2006.

Coale, K. H., Johnson, K. S., and Chavez, F. P., et al.: Southern Ocean Iron Enrichment Experiment: Carbon Cycling in High- and Low-Si Waters, Science, 304, 408–414, 2004.

Coale, K. H., Fitzwater, S. E., Gordon, R. M., Johnson, K. S., and Barber, R.T.: Control of community growth and export production by upwelled iron in the equatorial Pacific Ocean, Nature, 379, 621–624, 1996.

Cornell, R. M. and Schwertmann, U.: The Iron Oxides, Structure, Properties, Reactions, Occurrence and Uses, John Wiley, Hoboken, N. J, 2003.

Dentener, F. J., Carmichael, G. R., Zhang, Y., Lelieveld, J., and Crutzen, P. J.: Role of mineral aerosol as a reactive surface in the global troposphere, J. Geophys. Res., 101, 22 869–22 889, 1996.

Duce, R. A., Liss, P. S., and Merrill, J. T., et al.: The atmospheric input of trace species to the world ocean, Global Biogeochem. Cycles, 5, 193–259, 1991.

Falkowski, P. G.: Evolution of the nitrogen cycle and its influence on the biological sequestration of CO_2 in the ocean, Nature, 387, 272–275, 1997.

Fan, S.-M., Horowitz, L. W., Levy II, H., and Moxim, W. J.: Impact of air pollution on wet deposition of mineral dust aerosols, Geophys. Res. Lett., 31, L02104, doi:10.1029/2003GL018501, 2004.

Fan, S.-M., Moxim, W. J., and Levy II, H.: Aeolian input of bio-available iron to the ocean, Geophys. Res. Lett., 33, L07602, doi:10.1029/2005GL024852, 2006.

Fung, I. Y., Meyn, S. K., Tegen, I., Doney, S. C., John, J. G., and Bishop, J. K. B.: Iron supply and demand in the upper ocean, Glob. Biogeochem. Cyc., 14(1), 281-295, 2000.

Gao, Y., Fan, S.-M., and Sarmianto, J.: Aeolian iron input to the ocean through precipitation

ACPD

7, 10043–10063, 2007

scavenging: A modeling perspective and its implication for natural iron fertilization in the ocean, J. Geophys. Res., 108(D7), 4221, doi:10.1029/2002JD002420, 2003.
Goodman, A. L., Underwood, G. M., and Grassian, V. H.: A laboratory study of the heterogeneous reaction of nitric acid on calcium carbonate particles, J. Geophys. Res., 105, 29 053–29 064, 2000.
Hand, J. L., Mahowald, N. M., Chen, Y., Siefert, R. L., Luo, C., Subramaniam, A., and Fung, I.: Estimates of atmospheric-processed soluble iron from observations and a global mineral aerosol model: Biogeochemical implications, J. Geophys. Res., 109, D17205, doi:10.1029/2004JD004574, 2004.
Hanisch, F. and Crowley, J. N.: The heterogeneous reactivity of gaseous nitric acid on authentic mineral dust samples, and on individual mineral and clay mineral components, Phys. Chem. Chem. Phys., 3, 2474–2482, 2001.
Horowitz, L. W., Walters, S., and Mauzerall, D. L., et al.: A global simulation of tropospheric ozone and related tracers: Description and evaluation of MOZART, version 2, J. Geophys. Res., 108(D24), 4784, doi:10.1029/2002JD002853, 2003.
Intergovernmental Panel on Climate Change (IPCC), Climate Change 2001: The scientific Basis, Contribution of Working Group I to the Third Assesment Report of the Intergovernmental Panel on Climate Change, edited by J. T. Houghton et al., Cambridge Univ. Press, New York, 2001.
Jickells, T. D., An, Z. S., and Andersen, K. K., et al.: Global iron connections between desert dust, ocean biogeochemistry, and climate, Science, 308, 67–71, 2005.
JPL Publication 02-25: Chemical Kinetics and Photochemical Data for Use in Atmospheric Studies, Evaluation Number 14, Jet Propulsion Laboratory, California Institute of Technology, Pasadena, California, 2003.
Judeikis, H. S., Stewart, T. B., and Wren, A. G.: Laboratory studies of heterogeneous reactions of SO_2, Atmos. Environ., 12, 1633–1641, 1978.
Junge C. E.: The modification of aerosol size distribution in the atmosphere, Final Tech. Rep. Contract-Da 91-591-EVC 2979, US Army, 1964.
Kalnay, E., Kanamitsu, M., and Kistler, R., et al.: The NCEP/NCAR 40-year reanalysis project, Bull. Am. Meteorol. Soc., 77, 437–471, 1996.
Luo, C., Mahowald, N. M., Meskhidze, N., Chen, Y., Siefert, R. L., Baker, A. R., and Johansen, A. M.: Estimation of iron solubility from observations and a global aerosol model, J. Geophys. Res., 110, D23307, doi:10.1029/2005JD006059, 2005.

Martin, J. H., Coale, K. H., and Johnson, K. S., et al.: Testing the iron hypothesis in ecosystems of the equatorial Pacific Ocean, Nature, 371, 123–129, 1994.
Martin, S. T.: Precipitation and dissolution of iron and manganese oxides, in Environmental Catalysis, edited by V. H. Grassian, pp. 61-81, CRC Press, Coca Roton, Fla, 2005.
Meskhidze, N., Nenes, A., Chameides, W. L., Luo, C., and Mahowald, N.: Atlantic Southern Ocean productivity: Fertilization from above or below?, Global Biogeochem. Cycles, 21, GB2006, doi:10.1029/2006GB002711, 2007.
Meskhidze, N., Chameides, W. L., Nenes, A., and Chen, G.: Iron mobilization in mineral dust: Can anthropogenic SO_2 emissions affect ocean productivity?, Geophys. Res. Lett., 30(21), 2085, doi:10.1029/2003GL018035, 2003.
Meskhidze, N., Chameides, W. L., and Nenes, A.: Dust and pollution: A recipe for enhanced ocean fertilization?, J. Geophys. Res., 110, D03301, doi:10.1029/2004JD005082, 2005.
Ooki, A. and Uematsu, M.: Chemical interactions between mineral dust particles and acid gases during Asian dust events, J. Geophys. Res., 110, D03201, doi:10.1029/2004JD004737, 2005.
Seinfeld, J. H. and Pandis, S. N.: Atmospheric Chemistry and Physics, John Wiley & Sons, Inc., p. 537, 1998.
Spokes, L. J. and Jickells, T. D.: Factors controlling the solubility of aerosol trace metals in the atmosphere and on mixing into seawater, Aquatic Geochem., 1, 355–374, 1996.
Tie, X., Madronich, S., Walters, S., Edwards, D. P., Ginoux, P., Mahowald, N., Zhang, R., Lou, C., and Brasseur, G.: Assessment of the global impact of aerosols on tropospheric oxidants, J. Geophys. Res., 110, D03204, doi:10.1029/2004JD005359, 2005.
Usher, C. R., Al-Hosney, H., Carlos-Cuellar, S., and Grassian, V. H.: A laboratory study of the heterogeneous uptake and oxidation of sulfur dioxide on mineral dust particles, J. Geophys. Res., 107(D23), 4713, doi:10.1029/2002JD002051, 2002.
Vlasenko, A., Sjogren, S., Weingartner, E., Stemmler, K., Gäggeler, H. W., and Ammann, M.: Effect of humidity on nitric acid uptake to mineral dust aerosol particles, Atmos. Chem. Phys., 6, 2147–2160, 2006, http://www.atmos-chem-phys.net/6/2147/2006/.
Whitby, K. T.: The physical characteristics of sulfur aerosols, Atmos. Environ., 12, 135–159, 1978.
Zhu, X., Prospero, J. M., Millero, F. J., Savoie, D. L., and Brass, G. W.: The solubility of ferric ion in marine mineral aerosol solutions at ambient relative humidities, Mar. Chem., 38, 91–107,

1992.

ACPD

7, 10043–10063, 2007

Table 1. The uptake coefficients γ^* of HNO_3 and SO_2 on dust.

	γ_{HNO_3}	γ_{SO_2}
Base case	5×10^{-5} (RH<25%), 1×10^{-3} (RH>25%)	3×10^{-5} (RH<50%), 3×10^{-4} (RH>50%)
Ref case	5×10^{-6} (RH<25%), 5×10^{-5} (RH>25%)	3×10^{-6} (RH<50%), 3×10^{-5} (RH>50%)

*The aged γ is assumed to be the same as the initial one. The RH threshold of 25% for HNO_3 and 50% for SO_2 follows Fan et al. (2006). The variation range of γ_{SO_2} is 3×10^{-5}–1×10^{-3}, with the lower limit measured by Usher et al. (2002) and upper limit by Judeikis et al. (1978), who also examined the variation of γ_{SO_2} with relative humidity (RH). The variation range of γ_{HNO_3} is 5×10^{-5}–0.1, with the lower limit measured by Goodman et al. (2000) and upper limit by Hanisch and Crowley (2001). The measurement by Vlasenko et al. (2005) provides a RH dependence ofγ_{HNO_3}.

ACPD
7, 10043–10063, 2007

Table 2. Soluble Fe Flux to Each Major Oceanic Basin.

		North Indian	South Indian	North Pacific	South Pacific	North Atlantic	South Atlantic	Subarctic Pacific[d]	Tropical Pacific[e]	Southern Ocean[f]
Base case	[a]Sol flux	70.6	59.1	227	63.6	229	82.2	58.7	27.0	32.8
	[b]Sol flux	122	17.0	53.3	12.2	108	32.4	90.4	15.4	12.1
	[c]Solubility	3.2	8.3	17	13	5.2	3.6	18	26	4.8
Ref case	[a]Sol flux	122	56.2	280	53.4	328	84.2	68.8	32.3	18.9
	[b]Sol flux	211	16.1	65.9	10.3	154	33.2	106	18.4	6.94
	[c]Solubility	5.5	7.7	19	10	7.4	3.7	20	27	2.1

[a] Soluble Fe flux (10^9 g yr^{-1}) produced by having HNO_3, SO_2 and sulfate as the dust transformation agents;
[b] Soluble Fe flux in μmol m^{-2} yr^{-1};
[c] Fe solubility in percent;
[d] between 40 N–60 N and 150 E–130 W;
[e] between 10 S–10 N and 160 E–90 W;
[f] between 70 S–50 S.

ACPD
7, 10043–10063, 2007

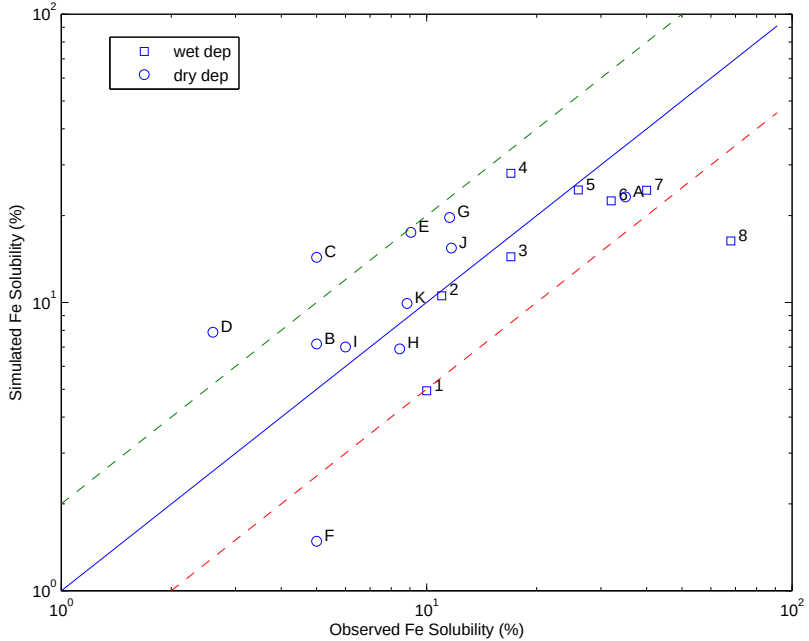

Fig. 1. Comparison of simulated and observed Fe solubility (%) for the Base case. Model results are monthly or annual means for long-term observations and averaged on the corresponding days and grid-box locations for cruises. Most of the observations are in Table 1 of Fan et al. (2006). We adopt the observations in Buck et al. (2006) for the Pacific instead of using Hand et al. (2004) that has the Fe(II) solubility. (1) NE Mediterranean (36.5 N, 34.25 E); (2) NW Mediterranean, (43.5 N, 4.5 E); (3) Britanny, France (47.8 N, 4.3 E); (4) Rhode Island, USA (42.0 N, 72.0 W); (5) North Carolina, USA (34.22 N, 77.86 W); (6) Dumont, Antarctic (65.0 S, 141.0 E); (7) Summit, Greenland (38.5 N, 72.5 W); (8) Bermuda (31.4 N, 64.1 W); A-D. Atlantic cruises (~26 N, 15 N: January–February; 5 N, 15 N: Jul-Aug); E. Pacific cruise (~22 N–50 N); F. Xi'an (~34 N, 109 E). G-H. Atlantic cruises (49 N-25 N, 21 N–5 N); I. Barbados (13.17 N, 59.43 W); J-K. Atlantic cruises (2 N–12 S, 16 S–43 S).

ACPD
7, 10043–10063, 2007

EGU

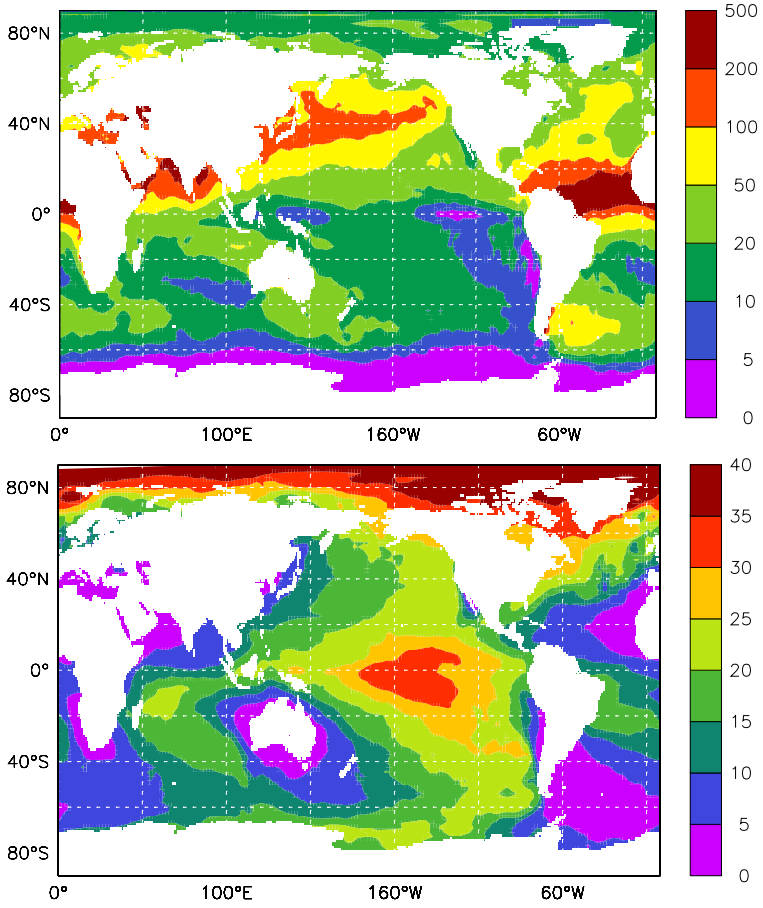

Fig. 2. Global distribution of **(a)** the annual mean soluble Fe flux (μmol m^{-2} yr^{-1}) and **(b)** Fe solubility (%) over the ocean.

ACPD
7, 10043–10063, 2007

EGU

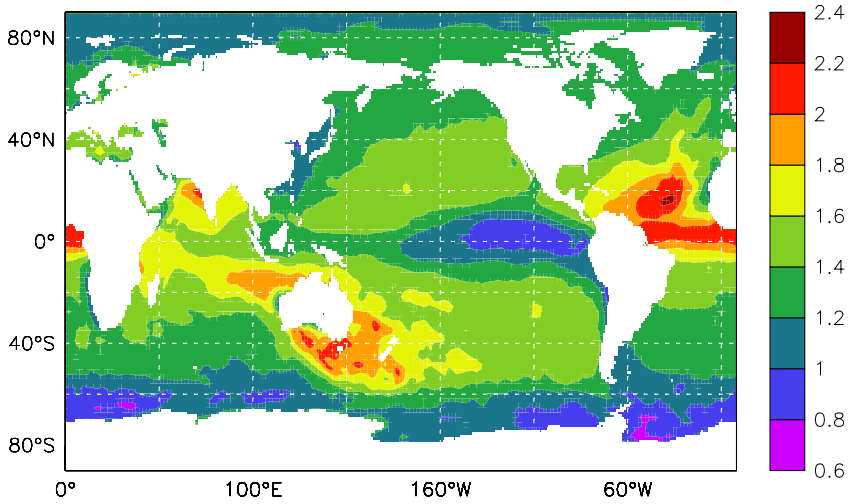

Fig. 3. Global distribution of the annual mean ratio of soluble Fe flux produced by HNO_3 versus that by SO_2 and sulfate (F_{23}) over the ocean.

ACPD
7, 10043–10063, 2007

EGU